

PACS: 42.65; 42.70; 61.70

Solid solutions of $\text{Cd}_x\text{Hg}_{1-x}\text{Te}:\text{V}:\text{Mn}$, $\text{Cd}_x\text{Hg}_{1-x}\text{Te}:\text{Ti}:\text{Mn}$ ($x = 0.9 - 0.95$): growth and properties

S.Yu. Paranchych, Yu.V. Tanasyuk, V.R. Romanyuk, O.S. Romanyuk, V.M. Makogonenko, M.D. Andriychuk, S.V. Synylo, Yu.I. Ivonyak

Yuriy Fedkovych Chernivtsi National University, 2 Kotsyubynskiy str., 58012 Chernivtsi, Ukraine
Phone: +380 (372)584753, fax: + 380 (372) 552914, E-mail: parsu@chnu.cv.ua

Abstract. Single crystals of $\text{Cd}_x\text{Hg}_{1-x}\text{Te}:\text{V}:\text{Mn}$, $\text{Cd}_x\text{Hg}_{1-x}\text{Te}:\text{Ti}:\text{Mn}$ ($x = 0.9-0.95$) with different concentrations of vanadium, titanium and manganese have been obtained via the modified Bridgman method and their optical, photoelectrical and galvano-magnetic properties have been studied. According to the performed investigations, the grown crystals proved to be satisfactorily homogeneous and highly sensitive within technically important spectral range of 1–1.5 μm . Energy position of vanadium and titanium level in the material under investigation determined from $R(T)$ dependence is of about 0.73–0.82 eV; 0.65–0.72 eV, respectively.

Keywords: semiconductors, crystal growth, 3d-impurities in semiconductor, galvanomagnetic effects.

Paper received 26.05.04; accepted for publication 21.10.04.

1. Introduction

Cadmium telluride is known to be one of the most intensively studied II-VI semiconductor compounds. Obtaining and investigation of cadmium telluride doped with 3d-elements are to a considerable extent stimulated by the possibility of its application in photodetectors, solar cells, IR-filters *etc.* CdTe and solid solutions of $\text{Cd}_x\text{Zn}_{1-x}\text{Te}$ ($x \approx 0.1$) on its base have already being used in X- and gamma-ray detectors for more than a decade [1, 2]. CdTe doped with 3d-elements reveals another important prospect for using it as photorefractive material in the near IR range where modern communication networks operate and most efficient solid state lasers irradiate.

At the present stage, a great number of scientific papers, e. g. [3–5], are devoted to growth and investigation of CdTe:3d. However, one of the key problems of the CdTe:3d based device production is preparation of highly sensitive crystals with stable characteristics. Moreover, one needs to search for some brand-new semiconductor materials that possess larger electron mobility values and exhibit, correspondingly, less time of photorefractive response. In this respect, solid solutions of $\text{Cd}_x\text{Hg}_{1-x}\text{Te}$ close to CdTe in their composition are considered as promising crystals.

In literature, we ran across the attempt to prepare highly resistive material of $\text{Cd}_x\text{Hg}_{1-x}\text{Te}:\text{Cl}$ ($x = 0.9$) from tellurium melt. However, according to Ref. [6] semi-in-

ulating properties were observed only in the latter, top portion of the crystalline bar. That is to say the matter of growth technology of 3d-doped CdTe and $\text{Cd}_x\text{Hg}_{1-x}\text{Te}$ still remains to be unsolved.

2. Experimental details

Single crystals of $\text{Cd}_x\text{Hg}_{1-x}\text{Te}:\text{V}:\text{Mn}$, $\text{Cd}_x\text{Hg}_{1-x}\text{Te}:\text{Ti}:\text{Mn}$ ($x = 0.9 - 0.95$) were grown via the Bridgman method in its two modifications. In the first case, the temperature gradient amounted to 15 K/cm and growing rate equaled 3.2 mm/h. In the second case, the former was of 2–3 K/cm, while the latter fell within the 0.5–0.8 mm/h range. To ensure a low value of temperature gradient both in axial and radial directions, gallium column was utilized. Zone rectified tellurium and cadmium were used as starting materials. A content of electrically active impurities was controlled over the whole length of zone rectified tellurium ingot through the measurements of an effective value of the Hall coefficient. The impurity concentration was found to range from $(6 \dots 8) \cdot 10^{14} \text{ cm}^{-3}$ to $(1 \dots 2) \cdot 10^{15} \text{ cm}^{-3}$. Purification of Cd was performed by zone melting in graphitized containers in the hydrogen atmosphere. Industrially pure 9N mercury was used in the experiments. A mixture of Cd, Te, Hg taken in their stoichiometric ratios along with carefully weighed V, Ti and Mn were loaded into 8 to 15 cm long quartz ampoules with 1.5 cm diameter. Such a sequence of loading enabled us to prevent cadmium interaction with mercury. To reduce heat

effect in the process of synthesis, dimensions of tellurium chops in the charge didn't exceed 10–15 mm². Concentrations of V, Ti and Mn doping impurities equaled $1 \cdot 10^{19} \text{ cm}^{-3}$.

Being evacuated down to $5 \cdot 10^{-5} \text{ mm Hg}$ and sealed, the quartz ampoules were placed into a synthesis furnace, temperature of which was increased according to the specially elaborated programme.

An appropriate temperature of synthesis for a certain composition was chosen following the relations given in [7]:

$$T_L (\text{°C}) = \frac{1000x}{1.37 + 0.97x} + 668,$$

$$T_S (\text{°C}) = \frac{1000x}{5.27 - 2.92x} + 668.$$

At the temperatures ranging from 723 – 773 K to 1115 – 1160 K, i.e. in the interval of the intensive synthesis reaction, the temperature was increased at the rate of about 1 K/min. On achievement of melting point, a rocking furnace was used to enhance the reaction between the components. After being kept at the melting point for 18 – 24 hours, the synthesized material was cooled down.

In order to carry out galvanomagnetic characterization of the obtained single crystals, the $2 \times 4 \times 8 \text{ mm}^2$ samples cut from different portions of the ingots were manufactured, while 1 mm thick wafers were prepared for optical and photoelectrical investigations.

Crystal homogeneity in the axial direction was studied by means of optical transmission investigations using MDR-23 and IRS-21 within the spectral range 0.8–2.5 μm .

3. Experimental results

According to the optical transmission spectra, the crystals grown at the temperature gradient of 15 K/cm and growth rate of 3.2 mm/h were somewhat inhomogeneous. In particular, all the samples exhibited slow decrease in the longwave transmission spectra. The optical transmission coefficient value varied within 40–60 % for different samples.

Fig. 1 shows curves of spectral distribution of optical transmission of the $\text{Cd}_x\text{Hg}_{1-x}\text{Te}:\text{V}:\text{Mn}$ ($x = 0.95$) crystal, $N_V = 1 \cdot 10^{19} \text{ cm}^{-3}$; $N_{\text{Mn}} = 1 \cdot 10^{19} \text{ cm}^{-3}$ in the axial direction. The crystal was grown at the minimum value of the temperature gradient. As one may notice, in this case the shortwave edges of the different samples almost overlap, which is indicative of sufficient homogeneity of the crystal. The achieved transmission values amounted to 65 %.

Absorption spectra of $\text{Cd}_x\text{Hg}_{1-x}\text{Te}:\text{Ti}:\text{Mn}$ ($x = 0.95$) single crystal, co-doped with concentrations of $N_{\text{Ti}} = N_V = 1 \cdot 10^{19} \text{ cm}^{-3}$, at 300 K are demonstrated in Fig. 2. For the samples manufactured from the bottom and top portions of the crystalline ingot, the band gap found from the $\alpha^2 = f(h\nu)$ dependence appeared to vary only by 0.045 eV, evidencing of good axial homogeneity of the crystal under investigation.

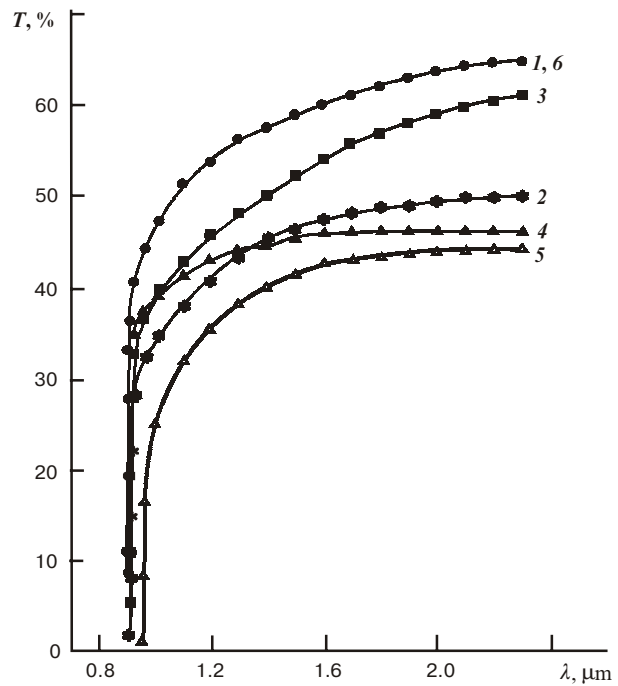


Fig. 1. Spectral distribution of transmission of the $\text{Cd}_x\text{Hg}_{1-x}\text{Te}:\text{V}:\text{Mn}$ samples ($x = 0.95$), grown via the Bridgman method at a minimum value of the temperature gradient (curve numeration corresponds to the beginning of solidification).

The experimental E_g value agreed well with that obtained from the expression $E_g = -0.25 + 1.59x + (5.233 \times 10^{-4} T [1 - 2.08x][0.328x^3])$, equalling 1.22 eV [8].

The optical absorption spectrum of $\text{Cd}_{0.96}\text{Hg}_{0.04}\text{Te}:\text{V}:\text{Mn}$, measured at 78 K, is given in Fig. 3 (curve 2). For comparison, in the same figure the absorption spectrum of $\text{CdTe}:\text{V}$ sample is illustrated (curve 1). This figure shows that for $\text{Cd}_{0.96}\text{Hg}_{0.04}\text{Te}$ the optical absorption edge is shifted toward the longwave region due to de-

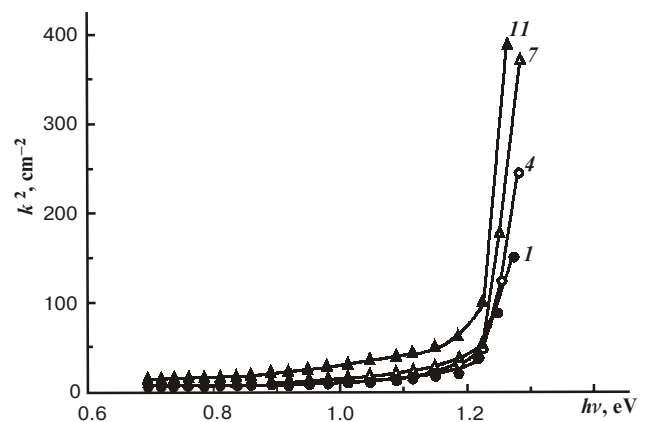


Fig. 2. Spectral dependence of the absorption coefficient of the $\text{Cd}_x\text{Hg}_{1-x}\text{Te}:\text{Ti}:\text{Mn}$ samples ($x = 0.95$) ($N_{\text{Mn}} = N_{\text{Ti}} = 1 \cdot 10^{19} \text{ cm}^{-3}$) (curve numeration corresponds to the beginning of solidification).

crease in the band gap. Some absorption bands appear in the optical absorption spectra of the crystals doped with V and Mn. These bands can be attributed to the intra-center absorption of V ions existing in different charge states as well as to photoionizing absorption.

According to [9], the absorption band at 0.8 eV in the low-energy region is attributed to the intra-center absorption between $^4T_1(F)$ and $^4A_2(F)$ vanadium charge states. At the same time, some increase in optical absorption is observed in the shortwave interval. This absorption isn't likely to be caused by its overlap with the fundamental absorption edge. The optical absorption increase within the 0.9-1.0 eV spectral range suggests the existence of V^{2+} and V^{3+} centers. Somewhat larger background absorption of $\text{CdHgTe}:\text{V}:\text{Mn}$ comparing to CdTe is mainly assigned to the scattering by crystal inhomogeneity resulting from non-uniform distribution of the components and impurity centers of V and Mn.

By this time, it's difficult to outline distinctly the role of Mn, but considering preliminary investigations the doping concentration of Mn influences the magnitude of photorefractive gain Γ .

Electrical characteristics of $\text{Cd}_x\text{Hg}_{1-x}\text{Te}:\text{Ti}:\text{Mn}$ ($x = 0.95$) samples are listed in Table 1.

Temperature dependences of Hall coefficient for $\text{Cd}_x\text{Hg}_{1-x}\text{Te}:\text{V}:\text{Mn}$ samples are shown in Fig. 4. Energy of vanadium level in $\text{Cd}_x\text{Hg}_{1-x}\text{Te}:\text{V}:\text{Mn}$ ($x = 0.9 - 0.95$) established from the $R(T)$ dependence is of about 0.73 – 0.82 eV. The hall mobility equaling to $(3.6 - 4) \cdot 10^2 \text{ cm}^2/\text{V}$ sec slightly fluctuates in the given temperature range. The number of the papers dealing with spectral dependences of photoconductivity arising in $\text{CdTe}:\text{V}$ is rather impressive [8–13]. E. g., the authors of [10] observed an increase in photoconductivity of $\text{CdTe}:\text{V}$ in the range of 0.82 – 1.4 μm at 300 K. The main band of photoconductivity was said to decrease at $h\nu < 1.1$ eV. In [13], it was reported on the existence of another band with its maximum at 1.1 eV revealed in the 123 K photoconductivity spectrum of $\text{CdTe}:\text{V}$ crystal with vanadium concentration in a liquid phase $1 \cdot 10^{19} \text{ cm}^{-3}$. The authors associate the occurrence of this band with photoionization of $\text{V}^{2+}_{\text{Cd}}$

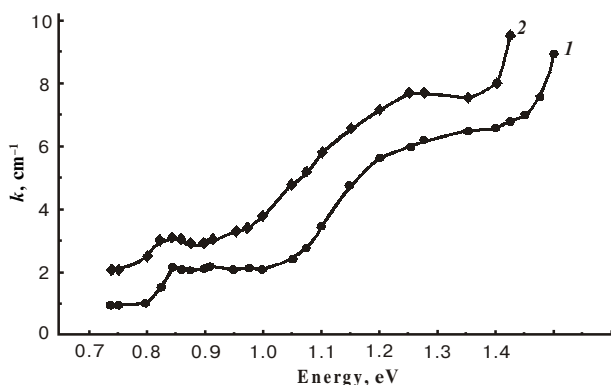


Fig. 3. Absorption spectra (78 K) of $\text{CdTe}:\text{V}$ (curve 1) and $\text{Cd}_{1-x}\text{Hg}_x\text{Te}:\text{V}:\text{Mn}$ ($x = 0.04$) (curve 2) doped with concentrations $N_V = 1 \cdot 10^{19} \text{ cm}^{-3}$, $N_{\text{Mn}} = 1 \cdot 10^{19} \text{ cm}^{-3}$.

SQO, 7(3), 2004

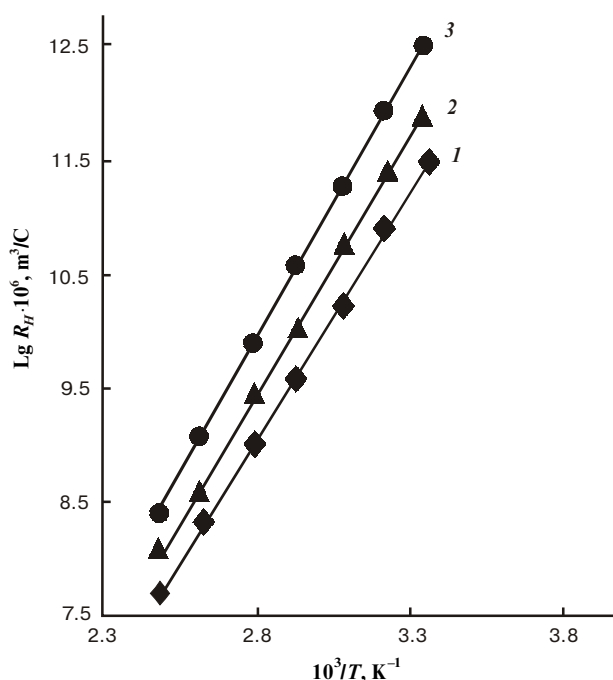


Fig. 4. Temperature dependence of the Hall coefficient: 1–2 – $\text{Cd}_x\text{Hg}_{1-x}\text{Te}:\text{V}:\text{Mn}$ ($x = 0.95$) $N_V = 1 \cdot 10^{19} \text{ cm}^{-3}$, $N_{\text{Mn}} = 1 \cdot 10^{19} \text{ cm}^{-3}$, 3 – $\text{Cd}_x\text{Hg}_{1-x}\text{Te}:\text{V}:\text{Mn}$ ($x = 0.9$) $N_V = 1 \cdot 10^{19} \text{ cm}^{-3}$, $N_{\text{Mn}} = 1 \cdot 10^{19} \text{ cm}^{-3}$.

ion via its $^4T_1(^4P)$ excited states. In Ref. [12], in addition to the spectral photoconductivity the optical absorption spectra of $\text{CdTe}:\text{V}$ at 80 K were investigated. They exhibited three absorption bands at 0.82, 0.51 and 1.24 eV, that were related to intra-central transitions to the excited states of $\text{V}^{2+}_{\text{Cd}}$ ion: $^4A_2(^4F)$, $^2E(^2G)$ and $^4T_1(^4P)$, respectively. Photoconductivity spectra resembled absorption ones, indicating all three states of $\text{V}^{2+}_{\text{Cd}}$ being resonant with the band ones. To our knowledge, investigations of $\text{Cd}_x\text{Hg}_{1-x}\text{Te}:\text{V}$, $\text{Cd}_x\text{Hg}_{1-x}\text{Te}:\text{V}:\text{Mn}$ photoconductivity spectra haven't been performed yet.

We have also studied spectral sensitivity of $\text{Cd}_x\text{Hg}_{1-x}\text{Te}:\text{V}:\text{Mn}$ samples ($x = 0.95$) with doping vanadium concentrations of $N_V = 5 \cdot 10^{19}$, $5 \cdot 10^{18} \text{ cm}^{-3}$ and $N_{\text{Mn}} = 1 \cdot 10^{19} \text{ cm}^{-3}$. The measurements were carried out on $2 \times 3 \text{ mm}^2$ samples produced from different parts of the wafers. The dark resistance of the samples ranging within $10^5 - 10^8 \Omega$ is changed under illumination by 10^2 to $5 \cdot 10^2$ orders of their magnitude. In Fig. 5, curves of photoconductivity spectral distribution for $\text{Cd}_x\text{Hg}_{1-x}\text{Te}:\text{V}:\text{Mn}$ ($x = 0.95$, $N_V = 5 \cdot 10^{19} \text{ cm}^{-3}$; $N_{\text{Mn}} = 1 \cdot 10^{19} \text{ cm}^{-3}$) are shown. As one may see, maxima of sensitivity and their halfwidths differ for the samples cut from the middle and edge parts of the wafer. Such a variation of sensitivity is thought to stem from segregation of components and impurities along the crystalline ingot in the process of its growth.

The presence of well pronounced maximum and sharp sensitivity decrease in the longwave region are typical for the samples fabricated from the middle part of the crystalline wafers of $\text{Cd}_x\text{Hg}_{1-x}\text{Te}:\text{V}:\text{Mn}$ ($x = 0.95$), $N_V = 5 \cdot 10^{18} \text{ cm}^{-3}$; $N_{\text{Mn}} = 1 \cdot 10^{18} \text{ cm}^{-3}$ (Fig. 5, b).

Table 1. Electrical characteristics of the $\text{Cd}_x\text{Hg}_{1-x}\text{Te}:\text{Ti}:\text{Mn}$ ($x = 0.95$) single crystals.

Index	n, cm^{-3}	$\rho, \Omega \cdot \text{cm}$	$\mu_H, \text{cm}^2/\text{V}\cdot\text{sec}$	Impurity activation energy, eV	Composition, x	Liquid phase impurity concentration $N_{\text{Ti}}, N_{\text{Mn}}, \text{cm}^{-3}$
1	$5.0 \cdot 10^8$	$2.0 \cdot 10^7$	631	0.72	0.96	$1.0 \cdot 10^{19}$
2	$4.4 \cdot 10^9$	$1.6 \cdot 10^6$	890	0.65	0.92	$1.0 \cdot 10^{19}$
3	$7.2 \cdot 10^8$	$1.6 \cdot 10^7$	546	0.71	0.95	$1.0 \cdot 10^{19}$

Concerning $\text{Cd}_x\text{Hg}_{1-x}\text{Te}:\text{Ti}:\text{Mn}$ ($x = 0.95$) single crystals, preliminary measurements of the resistance proved them to be low resistive in the central part of the single crystalline wafer (10^2 – $10^4 \Omega$), while the edge portion was characterized with high resistance falling into the range 10^7 – $10^8 \Omega$. The halfwidth and shape of spectral sensitivity appeared to be similar to those of $\text{Cd}_x\text{Hg}_{1-x}\text{Te}:\text{V}:\text{Mn}$ ($x = 0.95$) samples co-doped with concentrations $N_{\text{V}} = 5 \cdot 10^{18} \text{cm}^{-3}$; $N_{\text{Mn}} = 1 \cdot 10^{18} \text{cm}^{-3}$.

Proceeding from the undertaken investigations, it can be concluded that using the Bridgman method at small temperature gradients one may obtain semi-insulating,

sufficiently homogeneous and highly sensitive crystals of $\text{Cd}_x\text{Hg}_{1-x}\text{Te}:\text{V}:\text{Mn}$, $\text{Cd}_x\text{Hg}_{1-x}\text{Te}:\text{Ti}:\text{Mn}$. Considering transport properties of the investigated samples, one can assert that doping of $\text{Cd}_x\text{Hg}_{1-x}\text{Te}:\text{Ti}:\text{Mn}$ results in higher values of the charge carrier mobility with respect to the single crystals co-doped with V and Mn.

This work is performed with the support of Scientific Technological Center of Ukraine. Grant 2004.

References

1. Y. Eisen, Current state-of-the-art applications utilizing CdTe detectors // *Nuclear Instruments and Methods*, A **322**, pp. 596-603 (1992).
2. R.H. Redus, A.C. Huber, J.A. Pantazis, Improved thermoelectrically cooled X/γ-ray detectors and electronics // *Nuclear Instruments and Methods*, A **458**, pp. 214-219 (2001).
3. A.I. Strauss, The physical properties of cadmium telluride // *J. Rev. Phys. Appl.*, **12**(2), pp. 167-198 (1977).
4. J. L. Pautrat, J. M. Francou, N. Magnea, E. Molva, Saminadayar, Donors and acceptors in tellurium compounds // *J. of Crystal Growth*. **72**, pp. 194-204 (1985).
5. K.Y. Lay, N.C. Giles-Taylor, J.F. Schetzina, K.J. Bachmann, Growth and characterization of CdTe, $\text{Mn}_x\text{Cd}_{1-x}\text{Te}$, $\text{Zn}_x\text{Cd}_{1-x}\text{Te}$ and $\text{CdSe}_y\text{Te}_{1-y}$ crystal // *J. Electrochem. Soc.* **133**(5), pp. 1049-1051 (1986).
6. R. Triboulet, CdTe:Hg alloys crystal growth using stoichiometric zone passing techniques // *Rev Phys. Appl.*, **12**, pp. 123-128 (1977).
7. J. C. Brice, P. Capper, C. L. Jones, The phase diagramme of pseudobinary system CdTe-HgTe and segregation of CdTe // *J. of Crystal Growth*. **75**(2), pp. 395-399 (1986).
8. M.Y. Pines, O.M. Stafsudd, P.B. Bratt, Characterization of n-type mercury cadmium telluride // *J. Infrared Physics* **19**, pp. 633-638 (1979).
9. Yu.P. Gnatenko, R.V. Gamernyk, I.A. Faryna, V.S. Blazhkviv, A.S. Krochuk, Vanadium impurity states in cadmium telluride and zinc telluride // *Semiconductors* **30**(11), pp. 1975-1980 (1996).
10. J.C. Launay, V. Mazayer, M. Tapiero, J. P. Zielinger, Z. Gutllil, Ph. Delaye, G. Roosen, Growth, spectroscopic and photorefractive investigation of vanadium-doped cadmium telluride // *Appl. Phys. A: Solid and Surfaces*, **55**, pp. 33-40 (1992).
11. R.B. Bylsma, P.M. Bridenbaugh, D.H. Olson, A.M. Glass, Photorefractive properties of V-doped cadmium telluride // *Appl. Phys. Lett.*, **51**(12), pp. 889-891 (1987).
12. J.P. Zielinger, M. Tapiero, Z. Gutllil, G. Roosen, P. Delaye, J.C. Launay, Optical, photoelectrical, deep level and photorefractive characterization of CdTe:V // *Materials Science and Engineering B*, **16**, pp. 273-278 (1993).
13. E. Rzepka, A. Aoudia, M. Cuniot, A. Luson, Y. Marfaing, Optical and thermal spectroscopy of vanadium-doped CdTe and related photorefractive effect // *J. of Crystal Growth* **133**, pp. 244-248 (1994).

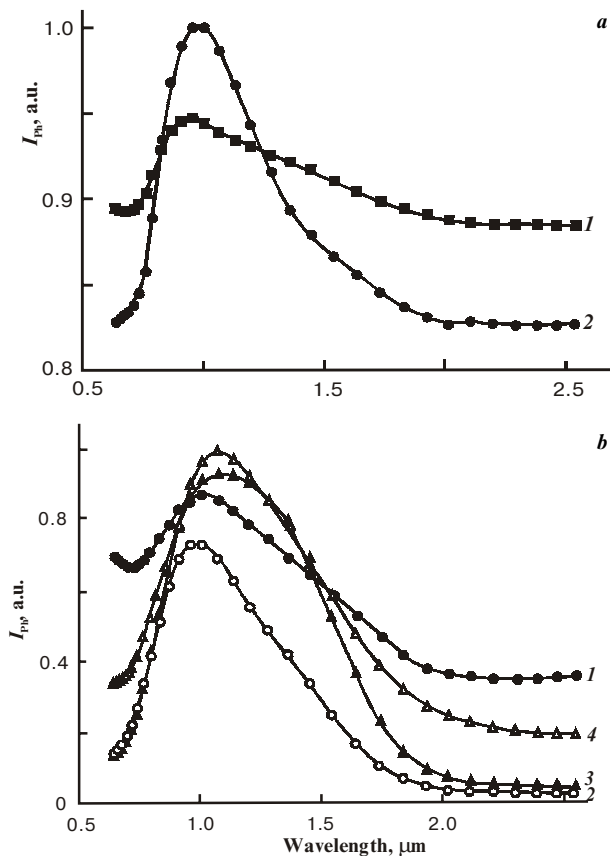


Fig. 5. Spectral distribution of photoconductivity of $\text{Cd}_{0.95}\text{Hg}_{0.05}\text{Te}:\text{V}:\text{Mn}$, (a) – $N_{\text{V}} = 5 \cdot 10^{19} \text{cm}^{-3}$, $N_{\text{Mn}} = 1 \cdot 10^{19} \text{cm}^{-3}$ (samples 1 and 2 were cut from the edge and central parts of the wafer), (b) – $N_{\text{V}} = 5 \cdot 10^{18} \text{cm}^{-3}$, $N_{\text{Mn}} = 1 \cdot 10^{18} \text{cm}^{-3}$ (Curve numeration is given according to the wafer position in the crystalline ingot, counting off from the beginning of crystallization.)